Plant, Cell and Environment (2008) **31**, 1214–1228 doi: 10.1111/j.1365-3040.2008.01826.x

$\delta^{18}O$ of water vapour, evapotranspiration and the sites of leaf water evaporation in a soybean canopy

LISA R. WELP[1], XUHUI LEE[1], KYOUNGHEE KIM[1], TIMOTHY J. GRIFFIS[2], KAYCIE A. BILLMARK[2] & JOHN M. BAKER[2,3]

[1]School of Forestry and Environmental Studies, Yale University, New Haven, CT 06511, USA, [2]Department of Soil, Water, and Climate, University of Minnesota, St. Paul, MN 55108, USA and [3]Agricultural Research Service, United States Department of Agriculture, St. Paul, MN 55108, USA

ABSTRACT

Stable isotopes in water have the potential to diagnose changes in the earth's hydrological budget in response to climate change and land use change. However, there have been few measurements in the vapour phase. Here, we present high-frequency measurements of oxygen isotopic compositions of water vapour (δ_v) and evapotranspiration (δ_{ET}) above a soybean canopy using the tunable diode laser (TDL) technique for the entire 2006 growing season in Minnesota, USA. We observed a large variability in surface δ_v from the daily to the seasonal timescales, largely explained by Rayleigh processes, but also influenced by vertical atmospheric mixing, local evapotranspiration (ET) and dew formation. We used δ_{ET} measurements to calculate the isotopic composition at the sites of evaporative enrichment in leaves ($\delta_{L,e}$) and compared that with the commonly used steady-state prediction ($\delta_{L,s}$). There was generally a good agreement averaged over the season, but larger differences on individual days. We also found that vertical variability in relative humidity and temperature associated with canopy structure must be addressed in canopy-scale leaf water models. Finally, we explored this data set for direct evidence of the Péclet effect.

Key-words: canopy scale; dew; evaporative site; non-steady state; oxygen isotopes and tunable diode laser; Péclet effect.

INTRODUCTION

Leaf transpiration transfers a significant portion of water from the soil to the atmosphere with consequences for regional humidity and precipitation patterns. In the central USA, the relative humidity has increased by 0.5–2.0% decade^{-1} from 1976 to 2004 (Dai 2006), and this may be partially attributable to increased agricultural productivity and crop density delivering more water to the atmosphere (Changnon, Sandstrom & Schaffer 2003). Transpiration is regulated by complicated interactions of plant physiology and environmental conditions; therefore, it is important to understand what controls leaf transpiration in the present climate, and also how these environmental factors and feedbacks may change in the future.

Correspondence: X. Lee. Fax: 203 432 5023; e-mail: xuhui.lee@yale.edu

The heavy isotope of oxygen, ^{18}O, is a valuable tracer of plant–atmosphere water interactions (e.g. Yakir & Sternberg 2000). During evaporation from leaves and the soil, the lighter $H_2{}^{16}O$ molecules evaporate more readily, leaving surface water pools more enriched in the heavy isotopologues ($H_2{}^{18}O$). The enrichment is linked in a predictable way to environmental conditions. Isotopic mass balance dictates that at the time scale of days to weeks, the isotopic composition of water transpired by leaves must be the same as water entering the plant from the soil at the rooting depth. This is referred to as the 'steady state'. At subdaily time scales, it is the difference between leaf water isotopic enrichment and δ_v that determines the diurnal change in the isotopic signature of transpiration (δ_T), reflecting short-term non-steady state (Dongmann *et al.* 1974; Harwood *et al.* 1998; Lee, Kim & Smith 2007).

The isotopic composition of precipitation has been studied globally for many years (IAEA/WMO 2004). In comparison, ecosystem water pools, such as soil, plant xylem and leaf water, are much more spatially variable and difficult to measure because traditional methods require separation of the water from the soil or organic matter (Ehleringer, Roden & Dawson 2000). For example, observations of bulk leaf water variability across seasons or among seasons are rare (Ometto *et al.* 2005; Pendall, Williams & Leavitt 2005). Leaf water enrichment is highly variable and may be estimated from measurements of environmental conditions using the Craig–Gordon model, assuming steady state where the isotopic composition of transpiration equals that of xylem water (Craig & Gordon 1965; Yakir & Sternberg 2000). However, a considerable number of investigators have found that the Craig–Gordon steady-state equilibrium prediction is approached only during midday in field conditions (e.g. Dongmann *et al.* 1974; Harwood *et al.* 1998; Cernusak, Pate & Farquhar 2002).

An increasing body of literature shows that in field conditions, the Craig–Gordon model predicts $\delta_{L,s}$ greater than $\delta_{L,b}$ (Dongmann *et al.* 1974; Bariac *et al.* 1989; Walker *et al.* 1989; Flanagan & Ehleringer 1991; Flanagan, Comstock &

Ehleringer 1991). There are two confounding issues at play here. Firstly, there is evidence that either discrete leaf water compartments containing unenriched source water or an isotopic gradient within the leaf caused by convection of source water by transpiration opposing the back-diffusion of water enriched in $H_2{}^{18}O$ from the site of evaporative enrichment leads to average leaf water more negative than $\delta_{L,s}$. The later process, known as the Péclet effect, is most important during midday when transpiration rates are large (Farquhar & Lloyd 1993). Secondly, δ_T may not equal δ_x especially during the transitional periods of the day as environmental conditions are changing rapidly (around sunrise and sunset). Lee *et al.* (2007) have shown that 24 h is too short to assume isotopic steady-state transpiration. Both the Péclet effect and the $\delta_T = \delta_x$ steady-state assumption will be explored in this paper.

Leaf water isotopic composition at the site of enrichment ($\delta_{L,e}$) not only controls δ_T, but also has consequences for other isotope tracers. For example, it plays a critical role in determining the oxygen isotopic composition of atmospheric CO_2 (Farquhar *et al.* 1993), and using this to partition net CO_2 fluxes into gross photosynthesis and respiration (Yakir & Wang 1996; Ogée *et al.* 2004), reconstructing past climate conditions from cellulose records, through $\delta_{L,e}$'s effect on $\delta_{L,b}$, (Epstein & Yapp 1977; Roden, Lin & Ehleringer 2000), and in paleostudies to estimate the ratio of marine to terrestrial biospheric productivity calculated from the Dole effect (Bender, Sowers & Labeyrie 1994; Hoffmann *et al.* 2004). Unfortunately, $\delta_{L,e}$ is not a directly measurable quantity. Measurements of δ_T, δ_v, accurate relative humidity with respect to the leaf temperature, and estimates of kinetic isotope fractionation allow us to infer the values of $\delta_{L,e}$ without invoking the steady-state assumption (Craig & Gordon 1965; Harwood *et al.* 1998).

The vapour phase δ_v and δ_T vary on even shorter time scales than bulk water pools. Traditional measurements used to resolve such variability are time-consuming because of the need to first condense the vapour to the liquid phase and then to perform mass spectrometer analysis (Helliker *et al.* 2002). Recent advances in mid-infrared spectroscopy have now made it possible to make high temporal resolution measurements of δ_v and transpiration δ_T in the surface layer (Lee *et al.* 2005), and also lower resolution measurements of δ_v throughout the upper troposphere and stratosphere on a global scale from satellites (Worden *et al.* 2006; Herbin *et al.* 2007).

In this study, we made near-continuous ecosystem-scale measurements of δ_v and δ_{ET} above a soybean canopy in Minnesota using tunable diode laser (TDL) technology. These observations also included periods of high humidity that allowed us to examine theoretical predictions in extreme environmental conditions. Our objectives were to: (1) quantify the temporal dynamics of the $\delta^{18}O$ composition of atmospheric water vapour and ecosystem water pools and the exchange fluxes over an entire season; (2) test the fundamental assumption that leaf water enrichment at the site of evaporation can be predicted using the Craig–Gordon steady-state model; and (3) test the Péclet effect at the canopy scale and under non-steady-state field conditions.

LIST OF VARIABLES

Variable	Description
C	molar density of water (mol m^{-3})
D	diffusivity of $H_2{}^{18}O$ in water (m^2 s^{-1})
E_S	soil evaporation (mol m^{-2} s^{-1})
E_T	transpiration (mol m^{-2} s^{-1}), assumed equal to ET
ET	evapotranspiration (mol m^{-2} s^{-1})
f	fractional enrichment of leaf water
h	humidity relative to the saturation vapour pressure at leaf temperature
I_{ET}	ET isoforcing (mmol m^{-2} s^{-1} ‰)
L_{eff}	effective diffusion length (m)
R_d	$^{18}O/^{16}O$ ratio of dew
R_{ET}	$^{18}O/^{16}O$ ratio of ET
T	temperature (°C or K)
v	water mixing ratio in the atmosphere [mmol (mol dry air)$^{-1}$]
x	molar mixing ratio of water isotopologue [e.g. mol $H_2{}^{18}O$ (mol dry air)$^{-1}$]
δ_d	$\delta^{18}O$ of dew (‰)
δ_{ET}	$\delta^{18}O$ of evapotranspiration (‰)
δ_g	$\delta^{18}O$ of ground water (‰)
$\delta_{L,b}$	$\delta^{18}O$ of bulk leaf water (‰)
$\delta_{L,e}$	$\delta^{18}O$ of leaf water at the site of evaporative enrichment calculated using δ_T measurements (‰)
$\delta_{L,s}$	$\delta^{18}O$ of leaf water at the site of evaporation calculated assuming steady-state conditions, $\delta_T = \delta_x$ (‰)
δ_P	$\delta^{18}O$ of precipitation (‰)
δ_s	$\delta^{18}O$ of soil water (‰)
$\delta_{storage}$	$\delta^{18}O$ of canopy storage of water vapour (‰)
δ_T	$\delta^{18}O$ of transpiration, assumed equal to δ_{ET} (‰)
δ_v	$\delta^{18}O$ of water vapour (‰)
$\delta_{v,e}$	$\delta^{18}O$ of liquid water in equilibrium with δ_v (‰)
δ_x	$\delta^{18}O$ of xylem water (‰)
ε_{eq}	equilibrium fractionation (‰)
ε_k	kinetic fractionation (‰)
$\wp$	Péclet number

THEORY

Departure from steady state

The isotopic composition of transpiration (δ_T) can be understood using theory developed for evaporating pools of water by Craig & Gordon (1965) (herein C&G), which describes the $\delta^{18}O$ of evaporation as a function of humidity, kinetic and equilibrium isotope fractionation, the isotopic composition of water of the evaporating surface, and atmospheric vapour. This relationship has been rearranged to solve for the isotopic composition of leaf water at the evaporating site ($\delta_{L,e}$). Here, we consider an approximation given by Farquhar & Lloyd (1993),

$$\delta_{L,e} = \delta_T + \varepsilon_{eq} + \varepsilon_k + h(\delta_v - \varepsilon_k - \delta_T), \quad (1)$$

where h is relative humidity referenced to leaf temperature, ε_{eq} is the temperature-dependent equilibrium fractionation factor between liquid and vapour (positive and in ‰) (Majoube 1971), and ε_k is a kinetic fractionation factor (positive and in ‰) following Farquhar, Ehleringer & Hubick (1989) and recently updated by Cappa *et al.* (2003),

$$\varepsilon_k = \frac{32r_s + 21r_b}{r_s + r_b} \quad (‰), \quad (2)$$

where r_s is stomatal resistance, and r_b is the leaf boundary layer resistance.

In this study, we used hourly measurements of δ_{ET} at the canopy scale to approximate δ_T, and then used Eqn 1 to calculate the isotopic composition of leaf water at the evaporating site ($\delta_{L,e}$). In agricultural ecosystems with high leaf area index (LAI), transpiration dominates ET. Therefore, δ_T equals δ_{ET} to a very close approximation when LAI is high (Shuttleworth & Wallace 1985). Stomatal resistance (r_s) was estimated from the Penman–Monteith equation for canopy resistance using eddy covariance and micrometeorologic measurements (Monteith 1965), and was converted from canopy scale to leaf scale by multiplying by half of the LAI. This method has the effect of weighting the canopy by sunlight penetration depth and compared well with LI-6400 leaf-level measurements from the upper and middle canopy. Boundary layer resistance (r_b) was estimated from canopy wind speed and leaf width (Gates 1980; Bonan 2002).

Equation 1 is commonly used to predict $\delta_{L,e}$ without directly measuring δ_T, but rather assuming steady-state evaporating conditions. At steady state, the water leaving the leaf has the same isotopic composition as xylem water (δ_x) entering the leaf (i.e. $\delta_T = \delta_x$). Substituting δ_x for δ_T in Eqn 1, we obtain a prediction of $\delta_{L,e}$ at the steady state ($\delta_{L,s}$),

$$\delta_{L,s} = \delta_x + \varepsilon_{eq} + \varepsilon_k + h(\delta_v - \varepsilon_k - \delta_x). \quad (3)$$

This approximation assumes that leaf water at the evaporating site instantaneously adjusts to changing environmental conditions such that outgoing δ_T equals incoming δ_x. However, the well-known diurnal cycle in $\delta_{L,b}$ requires that δ_T be less than δ_x in the morning as $\delta_{L,b}$ increases, and that δ_T be greater than δ_x in the evening as $\delta_{L,b}$ decreases, according to the isotopic mass balance inside the leaf. The steady state is reached during midday in the natural setting if the one-way water fluxes in and out of the leaf are high enough to keep up with rapidly changing environmental conditions. There is evidence that the steady state certainly does not apply at night when the one-way water fluxes are small (e.g. Cernusak *et al.* 2002; Farquhar & Cernusak 2005).

The relationship between $\delta_{L,e}$ and $\delta_{L,s}$ has been examined in relatively few experimental studies involving leaf chambers (Yakir *et al.* 1994; Harwood *et al.* 1998; Seibt *et al.* 2006). Here, we consider the difference $\delta_{L,e} - \delta_{L,s}$ as a measure of the departure from steady state. Similarly, the difference $\delta_T - \delta_x$, examined in detail by Lee *et al.* (2007) and Yakir *et al.* (1994), defines the non-steady-state behaviour. We can relate these two by taking the difference between Eqns 1 and 3,

$$\delta_{L,e} - \delta_{L,s} = (\delta_T - \delta_x)(1 - h). \quad (4)$$

Thus, observable differences between $\delta_{L,e}$ and $\delta_{L,s}$ occur only if δ_T deviates from δ_x and air is not saturated. In the special case when air approaches saturation ($h \to 1$), the difference between $\delta_{L,e}$ and $\delta_{L,s}$ vanishes as both values approach the isotopic composition of liquid in equilibrium with vapour ($\delta_v + \varepsilon_{eq}$). Because $\delta_{L,e}$ is a parameter of great interest, we will focus on the deviation of $\delta_{L,e}$ from steady state instead of δ_T.

The Péclet effect

Two issues confound the interpretation of the leaf water $\delta^{18}O$ measurements. Firstly, the commonly measured leaf water δ is for the bulk leaf water ($\delta_{L,b}$), but it is $\delta_{L,e}$ that exerts a direct influence on the isotope exchange of H_2O, CO_2 and O_2. The Péclet model captures the ratio of transpiration advection of unenriched xylem water to the diffusion of $H_2{}^{18}O$-enriched water from the evaporating sites within the bulk leaf lamina water. Proposed by Farquhar & Lloyd (1993), it allows us to relate $\delta_{L,e}$ to $\delta_{L,b}$ as

$$\delta_{L,b} - \delta_x = \frac{(\delta_{L,e} - \delta_x)(1 - e^{-\wp})}{\wp} \quad (5)$$

$$\wp = \frac{E_T L_{eff}}{CD},$$

where $\wp$ is the non-dimensional Péclet number, E_T is the transpiration rate of the leaf (mol m^{-2} s^{-1}), L_{eff} is an effective diffusion length (m), C is the molar density of water (55.6×10^3 mol m^{-3}), and D is the temperature-dependent diffusivity of the $H_2{}^{18}O$ in water (Cuntz *et al.* 2007). This model is the simplified longitudinal average of the more detailed Farquhar & Gan (2003) model and does not consider the enrichment of xylem water along the leaf.

Evidence supporting the Péclet effect has been indirect to date (Farquhar, Cernusak & Barnes 2007). In several cases, the agreement of modelled and measured $\delta_{L,b}$ was improved by including the Péclet effect in the leaf lamina and in some cases the xylem water in the leaf also (Cernusak *et al.* 2002; Farquhar & Gan 2003; Barbour *et al.* 2004; Cernusak, Farquhar & Pate 2005; Ripullone *et al.* 2008). According to Farquhar & Lloyd (1993), a positive correlation should exist between E_T and the fractional enrichment of leaf water (f),

$$f = (\delta_{L,b} - \delta_x)/(\delta_{L,e} - \delta_x). \quad (6)$$

As E_T increases, 1-f should increase in a curvilinear fashion (e.g. Fig. 4 of Barbour *et al.* 2004).

The second issue complicating the interpretation of the leaf water $\delta^{18}O$ is that in field conditions, the steady-state

assumption may be violated (Wang & Yakir 1995; Cernusak *et al.* 2002), and $\delta_{L,e}$ may not equal $\delta_{L,s}$. The Péclet effect can be quantified rigorously in the laboratory where steady state is achieved by holding environmental conditions constant, allowing $\delta_{L,e}$ to be identical to $\delta_{L,s}$ (Eqn 4). Cuntz *et al.* (2007) recently showed that Eqn 5 does not hold in the non-steady state, but still remains a reasonable approximation when $\delta_{L,b}$ is flux weighted for certain applications (also see Ogée *et al.* 2007).

Non-steady-state model of leaf water enrichment

Farquhar & Cernusak (2005) (herein F&C) included both of the previously discussed effects into a model of bulk mesophyll leaf water enrichment. They do not assume steady state, and treat $\delta_{L,b}$ and $\delta_{L,e}$ separately. We will test a few predictions of this model, including the backward calculation of $\delta_{L,e}$, using isotopic mass balance and the change in the measured $\delta_{L,b}$ (F&C Eqn 16) and the forward predictions of $\delta_{L,e}$ and $\delta_{L,b}$ (F&C Eqns 22 and 21, respectively).

MATERIALS AND METHODS

Site description

We measured δ_{ET} above a *Glycine max* (soybean) canopy from 30 May to 27 September 2006. The field, located at the University of Minnesota Rosemount Research and Outreach Center (RROC/UMORE PARK) just outside of Minneapolis-St Paul, MN, is currently managed as a conventional corn–soybean rotation. Many ongoing research activities aimed at quantifying carbon, water and energy fluxes at this site using eddy covariance and isotopic techniques have been documented elsewhere (Griffis *et al.* 2004, 2005b; Baker & Griffis 2005).

Climate conditions during the 2006 growing season are summarized in Table 1. The field was planted on 25 May and harvested on 10 October. The maximum LAI reached 8.2 at a full canopy height of about 1 m on 3 August. The field was not irrigated. Our TDL was installed on 1 June at the north edge of the field, with a fetch of 200–500 m in the 90–270 degree wind sector. The seasonal mean leaf water content was 110 g m^{-2} (mass of water per unit leaf area) based on weekly sampling.

Isotope measurements

Atmospheric δ_v was measured at two heights above the canopy by a TDL (TGA100, Campbell Scientific, Inc., Logan, UT, USA) from the absorbance spectra of $H_2{}^{16}O$ and $H_2{}^{18}O$. A dynamic calibration system, referred to as the 'dripper' described in Lee *et al.* 2005; Lee, Smith & Williams 2006, allowed us to correct for the non-linearity of the TDL measurement with respect to absolute water content by adjusting the mixing ratio of water in our calibration gases. The entire calibration procedure, including zero offset and gain corrections, and the approach used to minimize the non-linearity of the δ_v measurement is discussed in detail in Wen *et al.* (2008).

Canopy δ_{ET} was determined by the flux-gradient approach (Brunel *et al.* 1992; Yakir & Wang 1996; Wang & Yakir 2000), measuring the vertical gradients of water isotopologues at the two sampling heights as described and tested in Griffis *et al.* (2005b) and Lee *et al.* (2007). The height of the intakes increased over the season from 75 and 185 cm at the beginning to 108 and 198 cm by the end of the season to adjust for canopy growth. The molar $^{18}O/^{16}O$ isotope ratio of ET (R_{ET}) was calculated hourly as

$$R_{ET} = R_d \frac{x^{16}_{s,2} - x^{16}_{s,1}}{x^{18}_{s,2} - x^{18}_{s,1}} \frac{x^{18}_{a,2} - x^{18}_{a,1}}{x^{16}_{a,2} - x^{16}_{a,1}}, \quad (7)$$

where R_d is the molar ratio of the dripper calibration water, x is the mixing ratio of water isotopologues where the superscripts 16 and 18 denote the ^{16}O and ^{18}O molecules in water; s,1 and s,2 indicate span calibration vapour streams; and a,1 and a,2 represent ambient air sampled at heights 1 (upper) and 2 (lower). Note that when the vertical gradient in water vapour mixing ratio goes to zero, R_{ET} is undefined. The leading term, $R_d(x^{16}_{s,2} - x^{16}_{s,1})/(x^{18}_{s,2} - x^{18}_{s,1})$, is essentially a

Table 1. Monthly mean climate

Month	T (°C)	Rain (mm)	H_2O mixing ratio (mmol mol^{-1})	RH[a] (%)	Soil moisture (VWC[b]) 5 cm	10 cm	25 cm	Dew events[c] (% of nights)
May	15.7	47.2		(58)	0.25	0.32	0.38	(84)
June	20.6	48.6	15.5	64	0.21	0.27	0.35	60 (80)
July	24.3	64.7	21.0	67	0.21	0.26	0.32	81 (77)
August	20.7	145.6	19.7	80	0.23	0.28	0.35	84 (81)
September	14.4	73.3	13.7	78	0.26	0.31	0.35	54 (65)

[a]Relative humidity calculated from TDL-measured H_2O mixing ratio referenced to 3 m air temperature, mean of all data (day and night). Values in parentheses are from 3 m Viasala humidity sensor. Note that the TDL installation occurred at the beginning of June.
[b]Volumetric water content in units of volume of H_2O per volume of soil.
[c]Determined from the polarity of TDL H_2O vertical gradients: a higher mixing ratio at the upper level compared with the lower level indicates net downward water vapour flux or dew formation. Values in parentheses are from the sign of latent heat flux measurements.
TDL, tunable diode laser.

calibration factor that ranged from 1.10 to 1.35 over the season. The isotope ratios are reported using δ notation relative to the Vienna Standard Mean Ocean Water (V-SMOW) scale, $\delta = (R/R_{\text{V-SMOW}} - 1)$, in parts per thousand (‰) or per mil. The measured δ_v precision was approximately 0.2‰, and the δ_{ET} measurements achieved a precision of approximately 1.4‰ (Lee *et al.* 2007).

We were unable to directly measure and correct for the storage term in the flux isotope ratio calculation (Griffis *et al.* 2004) because there were no measurements of δ_v inside the canopy. An analysis of the rate of change of the ratio of the isotopologue fluxes of the lower intake was used as a surrogate for the canopy storage term ($\delta_{storage}$). There was no indication of a bias between δ_{ET} and $\delta_{storage}$ either seasonally or diurnally. We excluded δ_{ET} data associated with periods of poor fetch, rain events and measurement instability. After filtering δ_{ET}, we were able to account for 37% of the growing season hourly periods, an impressive total that would not be feasible without the TDL technology. Data recovery percentages for each month were 30% of June, 45% of July, 42% of August, and 32% of September.

We made daily $\delta^{18}O$ measurements of leaf water (at midday), with the centre vein removed, collecting ~4 large leaves from the upper and ~9 smaller leaves from the lower layers of the canopy separately from at least four different plants. We also made weekly measurements of xylem water, sampled at the base of the plant, and 10 cm soil water, event-based precipitation, and periodic measurements of groundwater. Plant and soil samples were sealed in glass vials and frozen until cryogenic water extraction using a vacuum line at Yale University. Extracted and bulk waters were analysed for $\delta^{18}O$ composition (precision = 0.2‰) using the CO_2 equilibration method on a GasBenchII autosampler attached to a Delta Plus XL isotope ratio mass spectrometer (Thermo Finnigan, Bremen, Germany) at Yale University.

Micrometeorological and eddy covariance measurements

Humidity was calculated in this experiment from the measured water mixing ratio from the TDL system above the canopy and was referenced to the saturation humidity at the desired temperature (e.g. air, leaf or soil). Canopy temperature was calculated from the measured outgoing long wave radiation, assuming an emissivity of 1.0. This produced values that agreed well with canopy temperature measurements from an Apogee IRTS-P sensor (Campbell Scientific, Inc.) before it failed early in the season, and was the canopy temperature used for all model calculations presented in this paper. Additional instrumentation at the site measured latent and sensible heat fluxes, net ecosystem exchange CO_2 flux, air and soil temperatures, wind speed, wind direction, and soil moisture (described in Griffis *et al.* 2004; Baker & Griffis 2005; Griffis, Baker & Zhang 2005a). The ET used for flux-weighting the δ_{ET} signal was calculated from the latent heat flux and gap filled using correlation with net radiation for the nearest 48 h.

Intensive measurement period

For a period of 72 h from 27 to 30 July (referred to as the intensive period), we collected leaf samples every 3 h, stem and soil (0, 5 and 10 cm depth) samples every 6 h, and 20 cm soil once per day. Shortly before sunrise, clean paper towels were used to wipe dew from the surface of leaves and were squeezed into a sample vial. Every 3 h, we measured leaf water content and leaf-level gas exchange properties using a LI-6400 (Li-Cor, Lincoln, NE, USA), including photosynthesis, transpiration, stomatal conductance and individual leaf temperature. Fetch was excellent during the entire intensive period. Leaf-level measurements were within the flux footprint of the TDL measurements.

RESULTS

Liquid water isotopic composition ($\delta_{L,b}$, δ_x, δ_s, δ_g, δ_P)

To provide context for interpreting the nearly continuous measurements of δ_v and δ_{ET}, we first present the measurements of the liquid water pools (Fig. 1a). Precipitation and soil waters showed moderate variability, and xylem water showed little variability over the season. Weekly measured δ_x usually fell between values of 10 cm δ_s and groundwater (δ_g), the latter of which showed very little deviation from the mean value of –10.00 ± 0.05‰. The most negative δ_x was measured 15 d after a large rain event that had a very negative δ_P.

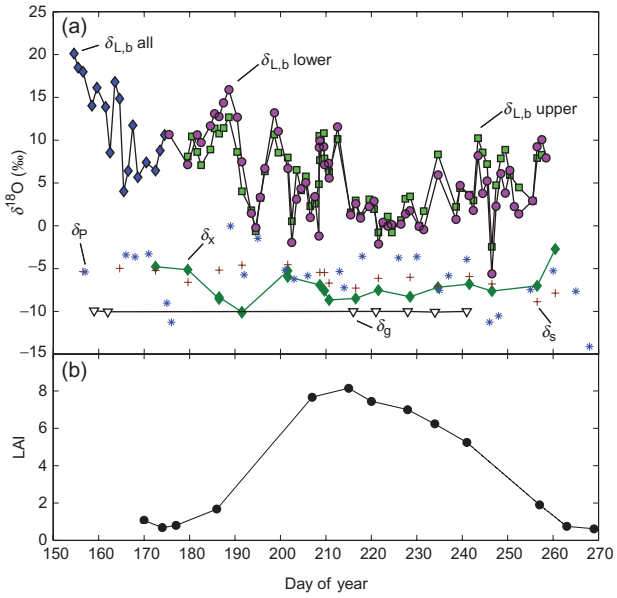

Figure 1. (a) Time series of ecosystem water pools. Groundwater (δ_g, upside-down open triangles), xylem (δ_x, green diamonds), 10 cm soil (δ_s, brown crosses), precipitation (δ_P, blue stars), bulk leaf water ($\delta_{L,b}$) sampled at midday from throughout the entire canopy (blue diamonds), upper canopy only (green squares) and lower canopy only (magenta circles). (b) Leaf area index (LAI) measured several times throughout the season (black circles) and linearly interpolated.

The largest variability, greater than 20‰, was observed in $\delta_{L,b}$. Early in the season, before day of year (DOY) 175, leaves were sampled from all heights in the developing canopy. As the canopy matured, upper and lower sections were sampled separately, with the centre veins removed. The most extreme $\delta_{L,b}$ enrichments of approximately 20‰ above δ_x were observed during the early part of the growing season. Variability in $\delta_{L,b}$ was strongly correlated with h (referenced to canopy temperature). A linear least squares fit equation including the upper and lower leaves over the growing season was $\delta_{L,b} = -26.5 \times h + 18.8$, with a coefficient of determination $R^2 = 0.75$ and number of observations $n = 136$.

Prior to DOY 200, but most pronounced between DOY 179 and DOY 192, the lower leaves showed greater midday $\delta_{L,b}$ values than the upper leaves; the pattern reversed after DOY 200. This surprising result leads us to hypothesize that canopy closure between planting rows around DOY 200 changed light, temperature and humidity characteristics of the lower canopy, but we do not have vertically resolved environmental measurements throughout the canopy to test this theory. By DOY 207, LAI was 7.7, close to the seasonal maximum of 8.2 (Fig. 1b). Transpired water enriching δ_v in the lower canopy cannot explain the depletion of the lower leaves relative to the upper leaves after DOY 200. The pattern was not symmetric at the end of the growing season, but neither is the canopy structure the same as the early season.

Seasonal and diurnal variability of δ_v

The $\delta^{18}O$ of water vapour (δ_v) contains insight into the seasonal, diurnal and synoptic variability in the hydrological cycle (Fig. 2). The daily mean δ_v during the growing season varied by nearly 15‰, with 5–10‰ changes over just a few days. The variability in daily mean δ_v was linearly correlated with daily mean air temperature ($R^2 = 0.51$, $n = 116$) and the natural log of the daily mean water vapour concentration (v, $R^2 = 0.66$, $n = 116$). This log-linear relation between δ_v and v from June to September was weaker at the hourly timescale ($\delta_v = 8.14 \ln(v) - 39.87$, $R^2 = 0.55$, $n = 5256$), but improved for daytime only conditions ($\delta_v = 8.99 \ln(v) - 42.9$, $R^2 = 0.71$, $n = 1541$). The largest deviations from the hourly best-fit function occurred during calm night-time conditions, when local ET enriched δ_v.

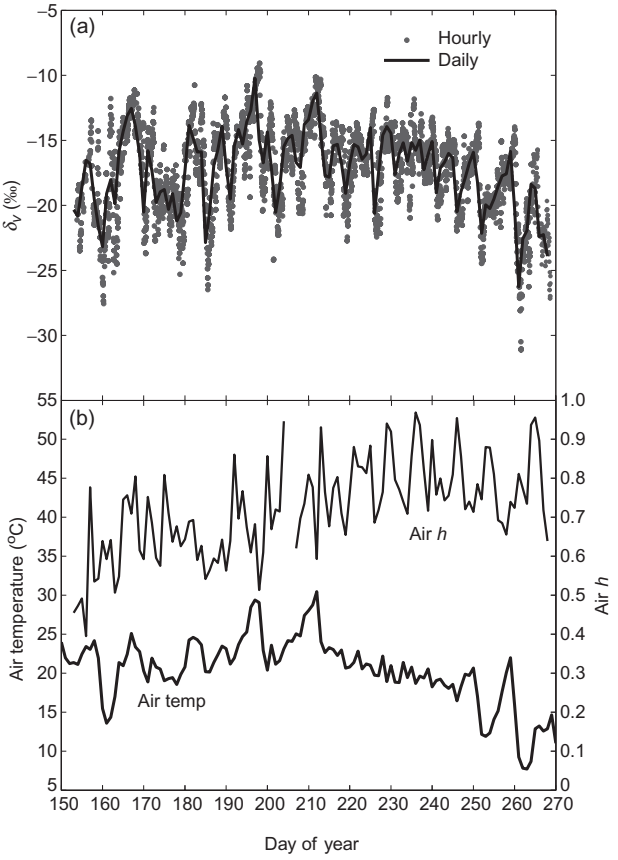

Figure 2. (a) Hourly mean δ_v (grey dots) and daily mean δ_v (black line) from the upper intake. (b) Daily mean air temperature measured at 3 m and relative humidity referenced to air temperature.

Monthly mean values of δ_v are listed in Table 2, along with the precipitation amount-weighted mean of δ_P. The correlation on an event basis between δ_P and liquid in equilibrium with δ_v ($\delta_{v,e}$) during rain events larger than 10 mm was excellent ($\delta_P = 1.07\ \delta_{v,e} + 1.23$, $R^2 = 0.98$, $n = 12$), giving us confidence in the accuracy of our δ_v measurements. Outside of rain events, monthly mean δ_v was not necessarily in equilibrium with precipitation, local soil water or stem water. In June and July, monthly mean δ_v was several ‰ more negative than the expected equilibrium with δ_P, but in

Table 2. Monthly mean $\delta^{18}O$ of water pools

Month	δ_v (‰)	δ_P[a] (‰)	$\delta_{v,e}$[b] (‰)	δ_x (‰)	δ_s (‰)	δ_{ET}[c] (‰)
May		–10.6				
June	–18.0	–6.4	–8.2	–5.0	–5.1	–3.5
July	–15.7	–5.2	–6.3	–7.6	–5.6	–5.3
August	–16.3	–6.5	–6.6	–7.6	–6.5	–4.3
September	–19.5	–9.3	–9.2	–5.8	–7.8	–6.4
June–September	–17.4	–6.8	–7.6	–6.5	–6.3	–4.8

[a]Weighted by amount of precipitation.
[b]Calculated from δ_v and monthly mean temperature from Table 1.
[c]Weighted by ET flux.
v, vapour; P, precipitation; v,e, liquid in equilibrium with vapour; x, xylem water; s, soil water at 10 cm; ET, evapotranspiration.

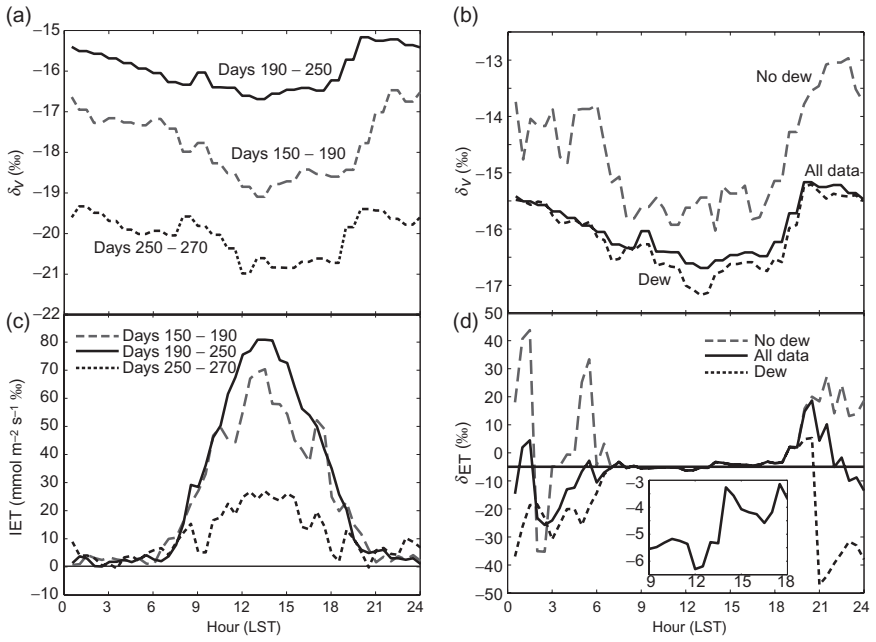

Figure 3. Ensemble mean diurnal cycles of δ_v filtered by (a) the time of the season; (b) DOY 190–250 was further filtered by the presence of dew on 51 nights and no dew on 10 nights. Similarly, (c) the isoforcing by evapotranspiration (ET) (I_{ET}) divided by season; and (d) δ_{ET} for the entire season filtered for periods of dew. Seasonal periods are divided into early (DOY 150–190), mid- (DOY 190–250) and late season (DOY 250–270) based on the crossover of leaf area index (LAI) = 3.

August and September, equilibrium conditions appeared to be satisfied (Table 2).

There was a persistent diurnal pattern to δ_v, with minimum values during the daytime and maximum values at night (1900–0200 h). Figure 3a shows daily ensemble means for three time periods during the season, early (DOY 150–190, LAI < 3), mid- (DOY 190–250, LAI = 3–8) and late season (DOY 250–270, LAI < 3). The shape of the diurnal cycle in δ_v for all three intervals was nearly identical with three main features: (1) a gradual decrease from 2100 to 1300 h; (2) a slight increase from 1300 to 1800 h; and (3) a larger, more rapid increase in the evening between 1800 and 2100 h. The early summer period showed the largest mean diurnal amplitude, 2.5‰ compared with 1.5‰ during the mid- and late growing season, and an extended evening increase in δ_v from 1800 to 2200 h. We hypothesized that local surface processes such as dew formation and canopy ET may contribute to the diurnal cycle in δ_v. The diurnal ensemble mean for the mid-season period was further divided into nights with and without dew formation (Fig. 3b). At this humid site, night-time dew formation was more common than no dew (Table 1). On nights lacking dew formation, δ_v appeared to remain fairly enriched until approximately 0600, and then decreased more rapidly than mornings following night-time dew. The potential influence of canopy ET is discussed in the next section.

Seasonal and diurnal variability of δ_{ET}

The ET flux-weighted monthly mean δ_{ET} was in the range of −3.5 to −6.4‰ (Table 2). Fig. 3d shows the ensemble mean diurnal cycle of δ_{ET}. For the daytime means, all data points were used. The night-time data were further screened by hourly observations with and without dew formation. At this humid site, night-time dew formation was more common than no dew (Table 1). During the daytime, δ_{ET} increased from 1000 to 1600 h by about 3‰ on average. Evening changes in δ_{ET} were over an order of magnitude larger than the daytime variation, as δ_{ET} approached infinity (positive or negative) at very low ET fluxes. In the case of no dew, δ_{ET} increased rapidly from 1600 to 2200 h and was quite variable, but mostly positive, after 2200 h. In the case of dew formation, however, the late afternoon/early evening values started to increase as in the case of no dew. Near 2100 h, δ_{ET} suddenly switched to very negative values, which was followed by a slow increase into early morning. The sudden switch to negative values occurred at the exact onset of dew formation on each night as the ET flux passed through zero. Examples of this switching can be seen during the intensive period (Fig. 4).

To quantify the effect of δ_{ET} on atmospheric δ_v, we calculated the ET isoforcing (I_{ET}) as

$$I_{ET} = ET(\delta_{ET} - \delta_v). \quad (8)$$

The diurnal ensemble mean I_{ET} was always positive, indicating that ET acted to enrich the atmosphere in $H_2{}^{18}O$ over the season and diurnally (Fig. 3c).

Non-steady-state nature of leaf $\delta^{18}O$

The slope of the regression of $\delta_{L,s}$ on $\delta_{L,e}$ was 0.97 ± 0.06 for the three-day intensive period and 0.90 ± 0.03 for days 190–250 (midday data). Close correlation between $\delta_{L,s}$ and $\delta_{L,e}$ results from the strong influence of h on both quantities, and a slope that is <1 demonstrates that $\delta_{L,s}$ is consistently less than $\delta_{L,e}$. We plotted the ensemble mean diurnal cycle for the dry canopy periods with high LAI, mid-July through August (Fig. 5) and also saw that the steady-state prediction

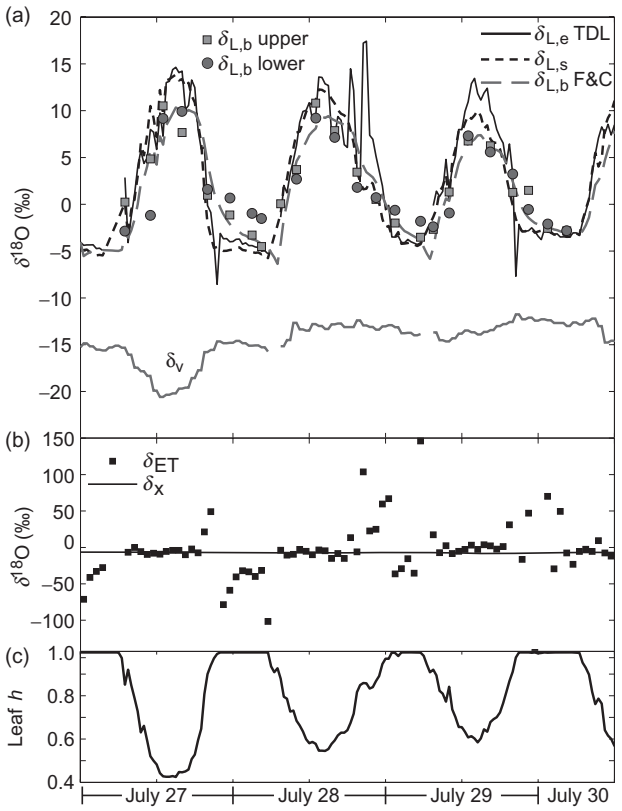

Figure 4. Observations during the intensive period. (a) Calculated $\delta_{L,e}$ using tunable diode laser (TDL) δ_{ET} measurements (solid black line) compared against the C&G steady-state calculations, $\delta_{L,s}$ (black dotted line) and $\delta_{L,b}$ F&C predictions (dashed grey line). Also shown are bulk leaf water from the upper canopy (light grey squares) and lower canopy (dark grey circles), and δ_v sampled at the upper intake (solid grey line). (b) Hourly δ_{ET} measurements and the mean of all δ_x samples collected during the intensive. (c) Relative humidity referenced to canopy temperature. C&G, Craig & Gordon; F&C, Farquhar & Cernusak.

consistently underestimated $\delta_{L,e}$. In calculating $\delta_{L,e}$ and $\delta_{L,s}$, we used the TDL measurement at the lower intake to determine δ_v and h.

The difference between $\delta_{L,e}$ and $\delta_{L,s}$ can also be examined on individual days during the intensive period (Fig. 4a). During saturated night-time conditions, the steady-state and non-steady-state values were identical as predicted by Eqn 4. The agreement between $\delta_{L,e}$ and $\delta_{L,s}$ was relatively good on 27 and 28 July, except for a few spikes in $\delta_{L,e}$ caused by outliers in the δ_{ET} measurement, but the two differed considerably on 29 July (Fig. 4a). This was surprising because the higher h on the third day should have reduced the offset between $\delta_{L,e}$ and $\delta_{L,s}$ according to Eqn 4. We believe that the larger departure on the third day may have been the result of water stress. There was no rain during the week proceeding the intensive period, and soil moisture decreased from 0.24 (m^3 H_2O m^{-3} soil) on 19 July, the day of the last rain event, to 0.20 on 29 July. Midday air temperatures ranged from 30–33 °C and incoming solar radiation was similar with clear sky conditions on all three days (Fig. 6a,b). Water stress was suggested by a morning stomatal conductance of 0.11 mol H_2O m^{-2} s^{-1}on 29 July, which was less than half of what it had been on 27 and 28 July (Fig. 6e). Similarly, the midday canopy-scale net CO_2 uptake measured by eddy covariance was also less on 29 July (17 μmol m^{-2} s^{-1}) than on 27 July (31 μmol m^{-2} s^{-1}) and 28 July (21 μmol m^{-2} s^{-1}) (Fig. 6c). Elevated $\delta_{L,e}$ compared with $\delta_{L,s}$ and low daytime CO_2 uptake continued after 29 July until the next rain event, on 2 August, brought the midday net CO_2 uptake back to previous stress-free levels (30 μmol m^{-2} s^{-1}). During another period of good fetch, from 6 to 9 July, when 20 days of no appreciable rain reduced soil moisture to nearly the lowest value of the entire season, (0.18), $\delta_{L,e}$ was also greater than $\delta_{L,s}$.

We also compared our estimate of $\delta_{L,e}$ from the TDL measurements with that calculated according to the system of equations in F&C (Fig. 7). The daytime agreement was good on the first two days of the intensive, but poor on the third day. At night, the F&C non-steady-state model prediction of $\delta_{L,e}$, using L_{eff} = 20 mm (black dotted line, F&C eqn 22), agreed better with that calculated from the leaf water ^{18}O mass balance (circles, F&C eqn 16) than our $\delta_{L,e}$ TDL measurements. However, in contrast to $\delta_{L,e}$ (TDL) and $\delta_{L,s}$ (C&G), neither of the F&C values returned to equilibrium with δ_v at times when air was saturated.

Péclet effect

As seen in Fig. 4a, midday $\delta_{L,b}$ was several per mil lower than $\delta_{L,e}$ during midday. This discrepancy has been attributed to the Péclet effect (see Theory section). To test this effect at the canopy scale, we sorted the data into five groups and estimated the leaf-level E_T by dividing canopy-scale ET by half of LAI (Fig. 8). This has the effect of

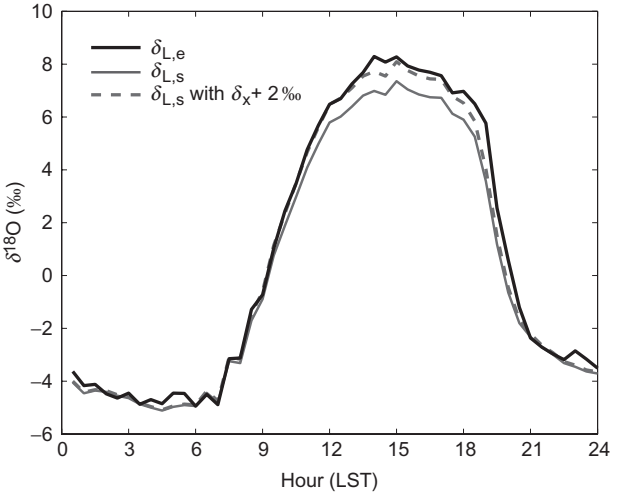

Figure 5. Diurnal ensemble means from mid-July through August of $\delta_{L,e}$ (solid black line), $\delta_{L,s}$ (solid grey line) and $\delta_{L,s}$ recalculated after adding 2‰ to δ_x (dashed grey line). $\delta_{L,e}$ was filtered for spikes by screening out $\delta_{L,e} - \delta_{L,s} > 5$‰ or <–5‰.

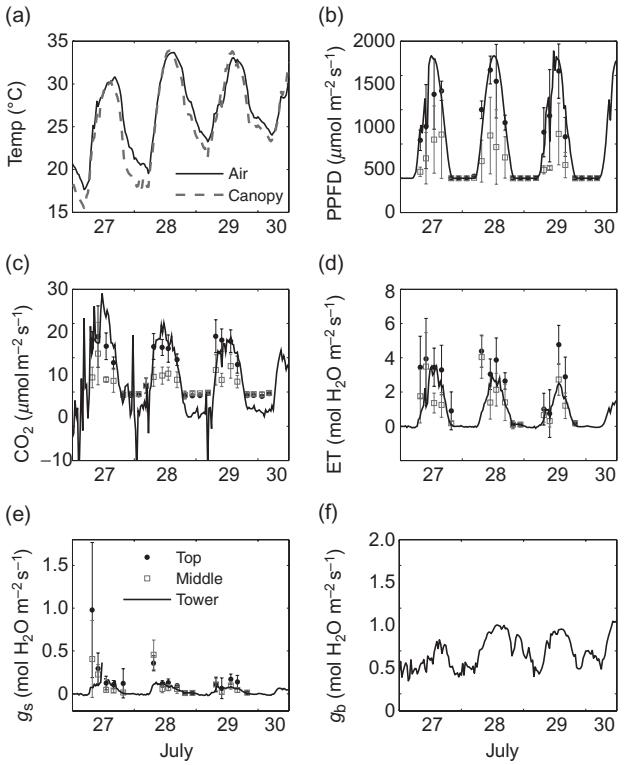

Figure 6. Tower and leaf-chamber measurements during the intensive period. (a) Air and canopy temperatures from the tower; (b) photosynthetic photon flux density (PPFD) above the canopy (solid line), at the leaf level, top of the canopy (black circles) and the middle of the canopy (grey squares); (c) canopy-scale net ecosystem production measured by eddy covariance (line) and leaf-level photosynthesis at the top and middle of canopy; (d) canopy-scale evapotranspiration (ET) divided by half leaf area index (LAI) (line) and leaf-level transpiration flux at the top and middle of canopy; (e) stomatal conductance (g_s) calculated in this study and leaf-level g_s from the chamber measurements; (f) estimated leaf-level boundary layer conductance (g_b). Error bars represent the standard deviation of replicate measurements on different plants.

weighting the canopy by sunlight penetration depth. The daytime fractional enrichment, f, fluctuated around 0.5, which is only halfway towards the theoretical limit of 0 (i.e. $1\text{-}f = 1$), and showed virtually no dependence at high E_T. Negative f values were observed at night during dew events, when $\delta_{L,b}$ was greater than $\delta_{L,e}$,. The value of L_{eff} implied by this data set is approximately 50 mm (Fig. 8b). We also show this analysis using $\delta_{L,s}$ instead of $\delta_{L,e}$ and arrive at the same $L_{eff} = 50$ mm. However, when we tuned the F&C-predicted $\delta_{L,b}$ against the observed leaf-level $\delta_{L,b}$ (Fig. 4), we arrived at a L_{eff} value of 20 mm instead.

Periods of dew formation

The dew water isotopic composition (δ_d) during the intensive campaign was close to the value of liquid water in equilibrium with δ_v ($\delta_{v,e}$). The difference between δ_d and both $\delta_{v,e}$ and the $\delta_{L,b}$ of upper leaves, measured between 0400 and 0500 h, was less than 1‰ on the first night and less than 0.4‰ on the second and third nights; thus, both dew water and the bulk leaf water in the upper canopy were in approximate equilibrium with water vapour, especially on the second and third nights (Table 3). Unlike the upper leaves that were covered by dew, many of the lower leaves remained dry because of higher temperature in the lower canopy, and the observed $\delta_{L,b}$ in the lower canopy was more positive relative to the upper canopy.

DISCUSSION

Temporal dynamics of δ_v

Seasonal and synoptic

Most of the seasonal variability in daytime δ_v could be attributed to Rayleigh distillation mechanisms (Gat 1996). The temperature and, more importantly, the water content of an air mass are indicators of its rainout history. At low temperatures, a large fraction of the original water vapour held by an air mass is condensed out, leaving relatively negative δ_v values. Previous studies based on TDL measurements have shown a similar log-linear relationship between atmospheric water mixing ratio and δ_v on an hourly timescale (Lee *et al.* 2007).

Diurnal

One might assume that the most obvious local influence on δ_v should be the ET isoforcing, which is strongly positive during the daytime and should increase δ_v (Fig. 3c). However, the δ_v daily minimum occurred during midday on average (Fig. 3a). A similar diurnal pattern was observed in

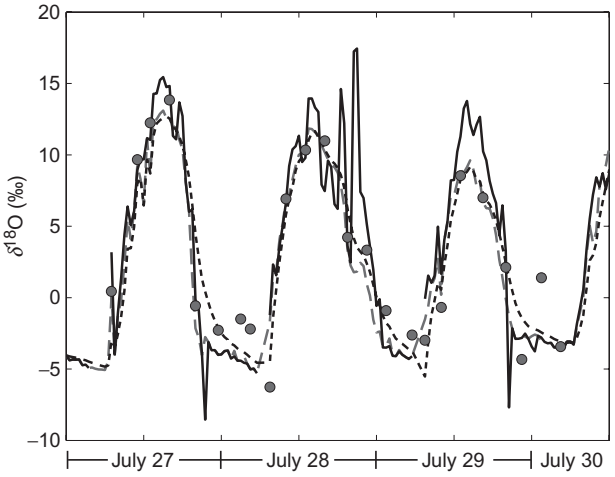

Figure 7. Comparison of $\delta_{L,s}$ (dashed grey line) and $\delta_{L,e}$ estimated in three different ways: from tunable diode laser (TDL) measurements (solid black line), the F&C back-calculation (grey circles) and the F&C forward prediction (dotted black line). Variable leaf water content was included in the model. $L_{eff} = 20$ mm and D was a function of temperature in the F&C forward prediction. Minimum $g_s = 0.04$ mol m^{-2} s^{-1}. F&C, Farquhar & Cernusak.

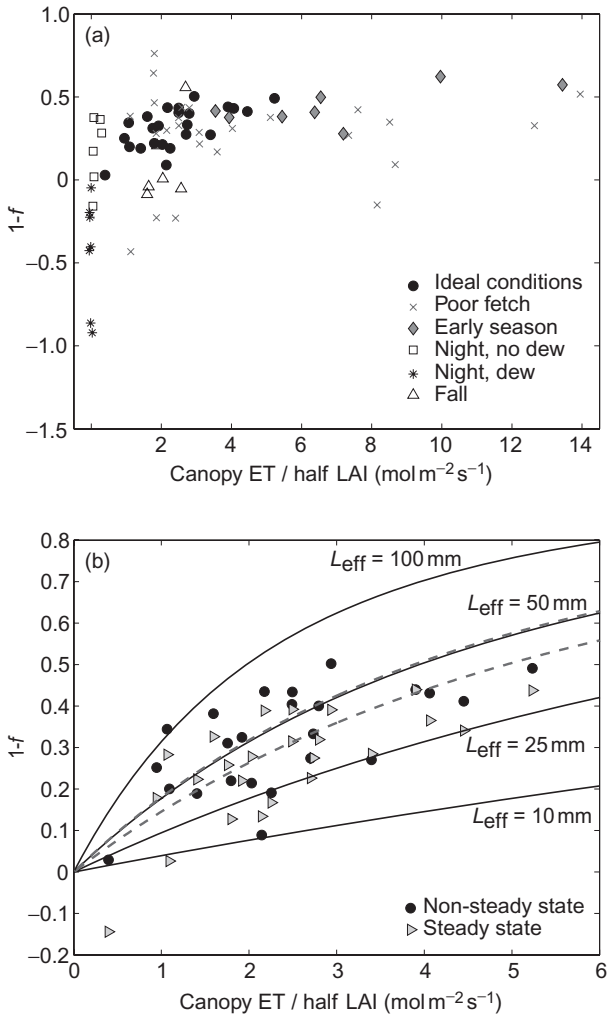

Figure 8. Fractional leaf water enrichment, or rather 1-*f*, versus leaf-level E_T [approximated as canopy evapotranspiration (ET) divided by half leaf area index (LAI)] of the upper leaves with centre veins removed. (a) The data are separated into six groups: ideal conditions – good fetch including daytime observations during the intensive and midday observations during the mid-growing season (DOY 191–242); poor fetch – midday observations with poor fetch; early season – midday data in the early season (DOY 181–188); night, no dew – night-time observations (1930–0730 h) during the intensive without dew; night, dew – night-time observations with dew during the intensive; and fall – midday data in the leaf senescence transition (DOY 244–258). (b) Ideal conditions only are compared with the Péclet model predictions using L_{eff} values of 10, 25, 50 and 100 mm with a mean *D* value from all the leaf collection times (solid black lines), as well as the maximum and minimum temperature range of *D* with L_{eff} = 50 mm (dashed grey lines), to show the range in the Péclet model calculations. Closed circles are for *f* calculated using $\delta_{L,e}$ (non-steady state), and open triangles are for *f* calculated using $\delta_{L,s}$ (steady state).

a high-frequency time series in New Haven, CT (Lee *et al.* 2006) and over two days of measurements in the Pacific Northwest (Lai *et al.* 2006). In the first case, the diurnal cycle was attributed to the diurnally variable sea breeze. In the second case, the morning decrease in δ_v was explained by entrainment of isotopically light water vapour from the free atmosphere with increased vertical mixing. An increasing contribution of enriched water transpired through the afternoon and evening returned δ_v to early morning values by 1900–2100 h. Another time series of δ_v from a temperate forest in New England showed no diurnal pattern (Lee *et al.* 2007). These previous studies suggest that the factors that control the diurnal cycle of δ_v may vary geographically.

At this site, it may be a combination of processes, such as dew, diurnally variable mixing in the boundary layer, and local ET, that drive the diurnal cycle of δ_v. There was evidence of local ET influence on δ_v in the evenings: the increase in δ_v from 1800 to 2100 h was timed exactly with an increase in δ_{ET} (Fig. 3a,b). The opposing effects of atmospheric mixing and the strength of ET isoforcing control the time change in δ_v. In midday periods, the mixed layer, typically 1 km deep in the Upper Midwest USA, mixes in more negative δ_v from the free troposphere, diluting the large surface ET isoforcing. During the sunset transition, the mixed layer usually collapses, and the rapidly increasing δ_{ET} signal was strong enough to influence the $H_2{}^{18}O$ budget of the surface layer air. Assuming a depth of 100 m for the mixed layer height during evening transitions, and typical ET, δ_{ET}, δ_v and *v* values, we estimated that the ET isoforcing can easily increase δ_v by 2‰ over 4 h. An increase of this magnitude, which is larger than the seasonal mean amplitude of 1‰, was indeed observed on nights with calm wind conditions.

Dew-free nights showed little change in δ_v from late evening until atmospheric turbulence increased in the morning. Assuming that the surface air mass is isolated from the upper free troposphere at night, condensation of ^{18}O-enriched water from the air could deplete δ_v as dew formed on the canopy surfaces. The evaporation of dew in the morning should enrich the surface air in $H_2{}^{18}O$, but the signal is presumably overwhelmed by the entrainment of more negative vapour by vertical mixing occurring at the same time. On any given day, however, synoptic variability in air mass trajectories may disguise these local effects. For example, the first day of the intensive period exhibited a midday minimum, but over the last two days, δ_v remained nearly constant.

Techniques for estimating δ_v

While accurate δ_v measurements are crucial to these types of water isotope studies, high-resolution measurements of δ_v are often impossible or impractical to make during field campaigns. White, Lawrence & Broecker (1994) recognized that studies ignoring δ_v are potentially flawed. A common assumption is that δ_v is in equilibrium with δ_x. However, we found that rarely was δ_v in equilibrium with δ_x at this site, and during midday δ_v was almost entirely decoupled from the surface δ_T (or δ_x). The equilibrium assumption resulted in errors of assimilation-weighted $\delta_{L,s}$ of 1.5–2.5‰ during our intensive measurement campaign. Using the noon value of δ_v on each day, and assuming it was constant over the

Table 3. Night-time microclimatic conditions and isotopic compositions of water pools during the intensive period

Day	δ_v (‰)	T_{surf}[a] (°C)	T_{air}[a] (°C)	δ_d (‰)	$\delta_{v,e}$[a,b] (‰)	δ_x (‰)	$\delta_{L,b\ (upper)}$[c] (‰)	$\delta_{L,b\ (lower)}$[c] (‰)
28 July	–14.9	18.4	20.8	–4.1	–5.0	–6.9	–4.5	–1.5
29 July	–13.6	22.6	24.0	–3.8	–4.0	–6.8	–3.5	–1.8
30 July	–12.5	24.4	25.4	–3.0	–3.1	–7.0	–2.8	–2.8

[a]Mean values of the last 5 h prior to δ_d and $\delta_{L,b}$ measurements.
[b]Calculated with respect to surface temperature.
[c]Measured between 0400 and 0500 h.

entire 24 h, reduces the error in assimilation-weighted $\delta_{L,s}$ to 0–1.5‰. Once-daily δ_v measurements, at least, are encouraged when $\delta_{L,s}$ is of interest.

If seasonally integrated signals are of interest, for example, in tree ring isotope studies, the Rayleigh distillation equation along with δ_P versus air temperature correlations and relative humidity time series can be used to estimate δ_v (Gat 1996). It is important to remember that δ_v predicted from δ_P versus air temperature regressions are for saturated vapour conditions (i.e. rain events) and are therefore positively biased during non-saturated conditions. Rayleigh distillation predicts that δ_v will be more negative during unsaturated conditions, with the difference depending on how dry the air mass is. Monthly mean δ_v during the low-humidity months of June and July was 1–2‰ more negative than equilibrium with δ_P would predict, whereas the more humid months of August and September were approximately in equilibrium with rain (Tables 1 & 2). These monthly mean δ_v results illustrate the importance of considering relative humidity when estimating δ_v from δ_P and air temperature.

The temporal dynamics of δ_{ET}

Monthly mean values

Assuming E_T is the dominant pathway of ET, we expected monthly mean δ_{ET} to closely match δ_x. The ET flux weighted monthly mean δ_{ET} was 0.8–3.3‰ higher than δ_x and was 0.3–2.2‰ higher than δ_s (Table 2). Generally speaking, a significant contribution from E_S should drive δ_{ET} more negative than δ_x, the opposite direction of our observations. Riley *et al.* (2003) showed that the isotopic forcing of soil evaporation may enrich δ_v in cases of strong evaporative enrichment of water in the surface soil layers. At this study site, we observed midday δ_s in the top 0–2.5 cm of the soil was enriched approximately 4‰ over the measurements at the 10 cm depth during the intensive campaign and then was nearly reset to deeper δ_s values at night. Enrichment in surface δ_s of this magnitude was not sufficient to result in a positive isoforcing by E_S. We suggest that the offset could be a result of mismatched footprints between our TDL measurement of δ_{ET} and the small plot area where we collected stem and soil samples for δ_x and δ_s analysis. The weekly δ_x and δ_s samples from one location may not capture the mean values for the entire TDL footprint. For example, a comparison with soil samples collected from another location in the same field showed that our routine measurements were on average 1.8‰ more negative. Our routine measurements were made in a portion of the field that was slightly depressed compared with the surrounding area. If the auxiliary site δ_s measurements were a more accurate representation of the entire tower flux footprint, the offset between δ_{ET} and δ_s and δ_x would almost entirely disappear. We show this by adding 2‰ to the C&G steady-state prediction in Fig. 5. This issue demonstrates the challenges of comparing measurements of varying footprints such as eddy covariance flux, TDL flux ratios, Keeling plots and plant-level measurements (e.g. Griffis *et al.* 2007). It also presents the challenge of estimating mean canopy-scale plant source water.

Additionally, there may be hidden sources of error in these new δ_{ET} gradient calculations. For example, this approach assumes that the eddy diffusivities of $H_2{}^{16}O$ and $H_2{}^{18}O$ are the same in air, but there have been no direct measurements supporting this assumption. Also, canopy storage effects may be accounted for in the future by measuring δ_v inside the canopy in addition to the gradient above the canopy.

Periods of dew formation

The sudden switching of δ_{ET} from strongly positive to strongly negative at the onset of dew formation occurred at the time when the water vapour flux passed from positive to negative (Figs 3d & 4b). During the intensive measurement, we observed that dew formation was confined to the upper canopy and that the lower canopy was warmed to a temperature above the dew point by heat released from the soil. Several recent papers have documented evidence of night-time transpiration (e.g. Barbour & Buckley 2007; Dawson *et al.* 2007; Fisher *et al.* 2007). Mass balance considerations show that when the component fluxes (downward dew flux versus upward transpiration flux from the lower canopy) occur in opposite directions, it is possible that the isotopic signal of the net flux is much larger in magnitude than those of the component fluxes. The highly variable δ_{ET} at night presents another challenge for the investigation of isotopic exchange in realistic field conditions.

The role of humidity in controlling leaf $\delta^{18}O$

Ambient δ_v exerts powerful influence on leaf water $\delta^{18}O$ (Roden & Ehleringer 1999). In high-humidity environments, $\delta_{L,e}$ approaches the liquid–vapour equilibrium with δ_v, as *h*

approaches unity (Eqn 1), and if saturation persists for long enough, the effect of back-diffusion will bring $\delta_{L,b}$ into an equilibrium state with δ_v as well (Table 3). Given that the majority of the nights at this study site experienced saturated conditions, it is critical to accurately measure δ_v when predicting $\delta_{L,e}$ (Table 1). Conversely, $\delta_{L,e}$ can be used as a record of δ_v in humid regions. This novel approach was recently described by Helliker & Griffiths (2007), who used an approximation of the $\delta_{L,e}$ signal preserved as cellulose $\delta^{18}O$ to reconstruct the δ_v of the atmosphere. In sub-saturation conditions, Barbour *et al.* (2004) showed that the sensitivity of $\delta_{L,e}$ to h increased as δ_v departs from equilibrium with δ_x.

On humid nights, the C&G model predicts that the asymptotic limit of canopy $\delta_{L,b}$ is $\delta_{v,e}$. Only when δ_x is identical to the equilibrium value of δ_v does $\delta_{L,b}$ approach δ_x. Our measurements show that δ_v and δ_x were not in equilibrium with each other on each of the three nights of the intensive period (Table 3) and were only on in equilibrium on a few fortunate days over the entire season.

Over the growing season, h plays a dominant role in $\delta_{L,b}$ variability as evidenced by the significant negative correlation between these two quantities. In our case, the highest $\delta_{L,b}$ was observed at the early growth stage when h and LAI were very low (Figs 1 & 2). At this time, the majority of solar radiation was consumed as sensible heat flux resulting in large surface temperatures. Even though h relative to saturation at the air temperature was similar to later periods, when expressed relative to the surface temperature, h in the early season was very low (0.1–0.3). The strong correlation with h emphasizes the importance of accurate humidity and surface temperature measurements when modelling leaf water isotopes.

Humidity may also explain the vertical gradient in $\delta_{L,b}$ between the upper and lower canopy and the switch in the relative difference midway through the season. Early in the season, when the plants were small, it is likely that radiative heating of the soil warmed the lower canopy and reduced h near the surface, such that $\delta_{L,b}$ was higher in the lower canopy than in the upper canopy. When the canopy density increased and filled in the areas between planting rows to form a closed canopy, h increased in the lower canopy relative to the upper canopy. At this point, upper canopy $\delta_{L,b}$ was greater than lower canopy $\delta_{L,b}$. Saurer, Siegwolf & Scheidegger (2001) reported that similar vertical patterns in $\delta_{L,b}$ were suggested by the $\delta^{18}O$ of cellulose. They found that the humidity increase in a closed canopy had a larger negative effect on the $\delta^{18}O$ of cellulose, through $\delta_{L,b}$, than the slight enriching effects of (1) increased kinetic fractionation via decreased wind speed and (2) enriched δ_v via increased transpiration contribution to canopy δ_v. Later in the season, the vertical pattern in $\delta_{L,b}$ did not reverse with the slow thinning of LAI because the overall canopy height and structure did not change drastically until senescence.

The steady-state assumption

The steady-state assumption – that δ_T equals δ_x – has been commonly used in isotopic partitioning studies to separate the influence of E_T and E_S from ET. Perhaps the biggest challenge in these studies is determining the transpiration flux-weighted δ_x from a heterogeneous ecosystem. Even though our relatively homogenous agricultural ecosystem was ideal for measuring canopy-scale δ_x, we were unable to show $\delta_T = \delta_x$ when flux-weighted over the season.

Several recent publications have pointed to the critical importance of using non-steady-state leaf water models to predict the $\delta^{18}O$ at the sites of evaporative enrichment for studies involving oxygen isotopes of CO_2 and O_2 (Farquhar & Cernusak 2005; Seibt *et al.* 2006; Lee *et al.* 2007). We expected that during the transitional periods of the day (sunrise and sunset), non-steady-state effects in $\delta_{L,e}$ would be more significant than in the middle of the day. Theoretically, δ_T should be lower than δ_x in the mornings as evaporative demand and $\delta_{L,b}$ increase. The opposite relationship should occur in the evening as $\delta_{L,b}$ decreases. Following to Eqn 4, $\delta_{L,e}$ should also be less than $\delta_{L,s}$ in the morning transition and greater than $\delta_{L,s}$ in the evening transition. After correcting for the possible error in canopy-scale δ_x in Fig. 5, there was no evidence of the transitional non-steady-state effect in the morning and a very slight indication of the evening non-steady state. Errors in the kinetic fractionation factor, δ_v and h resulting from the recycling of water in the canopy had no effect on the relative difference between $\delta_{L,e}$ and $\delta_{L,s}$ because the same terms appear in both Eqns 2 and 3. Within the uncertainty of the TDL measurement and footprint heterogeneity at the site, $\delta_{L,s}$ does appear to be a close approximation of $\delta_{L,e}$ when averaged over the season at least during the daytime. High night-time humidity at this site prevented an evaluation of the importance of non-steady state at night that has been suggested by several other studies in sub-saturation conditions (Farquhar & Cernusak 2005; Seibt *et al.* 2006).

The comparison of our TDL estimates of $\delta_{L,e}$ with the F&C model predictions was particularly interesting during the night (Fig. 7). F&C predictions were more positive than $\delta_{L,e}$ or $\delta_{L,s}$. The F&C back-calculation of $\delta_{L,e}$ from $\delta_{L,b}$ measurements included implicitly the diffusion between the sites of enrichment and the larger volume of mesophyll water with a slow isotopic turnover time. The F&C forward prediction of $\delta_{L,e}$ also incorporates this slow isotopic turnover. Neither prediction settled to equilibrium with δ_v at times when air was saturated as demanded by Eqn 1. More night-time measurements are needed to resolve these differences.

During the intensive period, midday $\delta_{L,s}$ was closer to $\delta_{L,e}$ on the first two days (27 and 28 July) than on the third day (29 July) (Fig. 4). The departure of $\delta_{L,e}$ (and δ_T) from $\delta_{L,s}$ (and δ_x) on the third day may have been the result of water stress. The mechanistic link between the non-steady-state behaviour and drought stress is, however, not fully understood. Drought stress may result in changes of the volumetric leaf water content and a time-varying L_{eff} in the Péclet effect calculation (Cuntz *et al.* 2007). How to incorporate these factors into theoretical models to predict δ_T is an area for future research.

Péclet effect

Our measurements of $\delta_{L,e}$ allowed us to test the Péclet effect during natural field conditions. The predicted curvilinear relationship with transpiration was observed, albeit with large scatter (Fig. 8a). We used this data to estimate a L_{eff} value of approximately 50 mm (Fig. 8b). Cuntz *et al.* (2007) showed that this relationship should not hold in the non-steady state; however, our midday leaf sampling strategy should tend towards steady-state conditions on each individual day. The lack of perfect agreement suggests that additional parameters may be needed to fully resolve the differences in the Péclet effect and gas exchange properties between the leaf scale and the canopy scale.

This analysis was complicated by comparing across the leaf and canopy scales. As previously noted, $\delta_{L,e}$ was derived from δ_T at the canopy level, where $\delta_{L,b}$ was measured at the plant level. For this reason we also compared the Péclet effect using $\delta_{L,s}$ derived from δ_x measured at the plant level. There is considerable error in our estimate of leaf-level transpiration from the canopy ET eddy flux measurement that greatly affects the best-fit value of L_{eff} that we solved for in Fig. 8b. Also, uncertainty in the estimates of r_b can easily change ε_k by 0–5‰ depending on the formula used from the literature (Bonan 2002).

Using the same method for estimating leaf-level transpiration (canopy ET/half LAI) during the intensive campaign in F&C eqn 22 led to an estimate of $L_{eff} = 20$ mm by matching $\delta_{L,b}$ observations. This discrepancy is partly caused by the difference in $\delta_{L,e}$ from TDL measurements (resulting in $L_{eff} = 50$ mm) and F&C's forward prediction, which includes the Péclet effect in $\delta_{L,e}$ (resulting in $L_{eff} = 20$ mm). These L_{eff} values are also solved for different time periods, the three-day intensive and averaged over the entire season. Regardless, L_{eff} values of 20–50 mm are both within the range estimated for wheat by Barbour *et al.* (2004). However, they could be considerably lower if we took into account xylem and veinlet enrichment inside the leaves (Ripullone *et al.* 2008).

In the evenings when air became saturated, $\delta_{L,e}$ quickly decreased to $\delta_{v,e}$ according to Eqn 3. The highly enriched $\delta_{L,b}$ decreased more slowly than $\delta_{L,e}$ because of the slow molecular diffusion of $H_2{}^{18}O$ in the bulk leaf water. In such transitional periods, $\delta_{L,e}$ was lower than $\delta_{L,b}$, causing 1-*f* to become negative. A negative 1-*f*, or more generally, the tendency for $\delta_{L,b}$ to reach equilibrium with the ambient vapour shows that there existed an isotopic exchange of $H_2{}^{18}O$ between leaves and the air, perhaps through a partially open stomatal pathway (Barbour & Buckley 2007; Dawson *et al.* 2007) even when air was at saturation and the net water vapour flux was small. Negative night-time values of 1-*f* were also shown by Barnard *et al.* (2007).

CONCLUSIONS

Continuous canopy-scale isotope measurements made possible by TDL technology have the potential to improve our mechanistic understanding of atmosphere–plant gas exchange on a timescale relevant to natural changing environmental conditions. Several unique oxygen isotope time series were presented in this paper, including long-term measurements of δ_{ET} that showed that the influence of the ET isoflux on δ_v was overwhelmed by vertical atmospheric mixing during midday, but contributed more significantly to observations in the evenings. Comparing high-frequency calculations of $\delta_{L,e}$ with steady-state predictions showed good agreement when averaged over the season. Our measurements also identify new features that are unique to the canopy scale and have been unobservable in laboratory and leaf chamber experiments: (1) daily measurements of $\delta_{L,b}$ pointed to vertical gradients in *h* that changed from increasing with height to decreasing with height midway through the growing season, a result of canopy structure effects on *h* (i.e. canopy closure); (2) the onset of dew formation caused abrupt switches in δ_{ET} from large positive values to large negative values; (3) accurate δ_v measurements are crucial if ($\delta_{L,b}$ or $\delta_{L,e}$ are parameters of interest; and (4) the above-mentioned data sets ($\delta_{L,b}$, $\delta_{L,e}$ and E_T rates) created an opportunity to test the Péclet effect during non-steady-state field conditions. While the theory did not exactly match observations, there was some evidence for decreasing leaf water enrichment at high E_T rates. These results shed insights into the factors controlling $\delta_{L,e}$ and δ_T, which are important variables used in global H_2O, CO_2 and O_2 cycle research. Field observations such as these present an excellent test for canopy-scale ecosystem models that incorporate water isotope tracers.

ACKNOWLEDGMENTS

This work was supported by the National Science Foundation grants EAR-0229343, DEB-0514904 and DEB-0514908. We thank the University of Minnesota's UMORE PARK for providing the infrastructure necessary for this study, Travis Bavin for his help during the intensive period, and Poorva Gupta and Yale's ECSIS lab for assisting with water extractions and isotope analysis. We also thank Graham Farquhar and two anonymous reviewers for thoughtful comments on the manuscript.

REFERENCES

Baker J.M. & Griffis T.J. (2005) Examining strategies to improve the carbon balance of corn/soybean agriculture using eddy covariance and mass balance techniques. *Agricultural and Forest Meteorology* **128,** 163–177.

Barbour M.M. & Buckley T.N. (2007) The stomatal response to evaporative demand persists at night in *Ricinus communis* plants with high nocturnal conductance. *Plant, Cell & Environment* **30,** 711–721.

Barbour M.M., Roden J.S., Farquhar G.D. & Ehleringer J.R. (2004) Expressing leaf water and cellulose oxygen isotope ratios as enrichment above source water reveals evidence of a Péclet effect. *Oecologia* **138,** 426–435.

Bariac T., Rambal S., Jusserand C. & Berger A. (1989) Evaluating water fluxes of field-grown alfalfa from diurnal observations of natural isotope concentrations, energy budget and ecophysiological parameters. *Agricultural and Forest Meteorology* **48,** 263–283.

Barnard R.L., Salmon Y., Kodama N., Sorgel K., Holst J., Rennenberg H., Gessler A. & Buchmann N. (2007) Evaporative enrichment and time lags between delta O-18 of leaf water and organic pools in a pine stand. *Plant, Cell & Environment* **30,** 539–550.

Bender M., Sowers T. & Labeyrie L. (1994) The dole effect and its variations during the last 130 000 years as measured in the Vostok ice core. *Global Biogeochemical Cycles* **8,** 363–376.

Bonan G. (2002) *Ecological Climatology: Concepts and Applications*. Cambridge University Press, Cambridge, UK.

Brunel J.P., Simpson H.J., Herczeg A.L., Whitehead R. & Walker G.R. (1992) Stable isotope composition of water-vapor as an indicator of transpiration fluxes from rice crops. *Water Resources Research* **28,** 1407–1416.

Cappa C.D., Hendricks M.B., DePaolo D.J. & Cohen R.C. (2003) Isotopic fractionation of water during evaporation. *Journal of Geophysical Research-Atmospheres* **108,** 4525, doi:4510.1029/2003JD003597.

Cernusak L.A., Pate J.S. & Farquhar G.D. (2002) Diurnal variation in the stable isotope composition of water and dry matter in fruiting *Lupinus angustifolius* under field conditions. *Plant, Cell & Environment* **25,** 893–907.

Cernusak L.A., Farquhar G.D. & Pate J.S. (2005) Environmental and physiological controls over oxygen and carbon isotope composition of Tasmanian blue gum, *Eucalyptus globulus*. *Tree Physiology* **25,** 129–146.

Changnon D., Sandstrom M. & Schaffer C. (2003) Relating changes in agricultural practices to increasing dew points in extreme Chicago heat waves. *Climate Research* **24,** 243–254.

Craig H. & Gordon L.I. (1965) *Deuterium and oxygen-18 variations in the ocean and the marine atmosphere*. Paper presented at the Proceedings of a Conference on Stable Isotopes in Oceanographic Studies and Paleotemperatures, Spoleto, Italy, 26–30 July.

Cuntz M., Ogée J., Farquhar G.D., Peylin P. & Cernusak L.A. (2007) Modelling advection and diffusion of water isotopologues in leaves. *Plant, Cell & Environment* **30,** 892–909.

Dai A.G. (2006) Recent climatology, variability, and trends in global surface humidity. *Journal of Climate* **19,** 3589–3606.

Dawson T.E., Burgess S.S.O., Tu K.P., Oliveria R.S., Santiago L.S., Fisher J.B., Simonin K.A. & Ambrose A.R. (2007) Nighttime transpiration in woody plants from contrasting ecosystems. *Tree Physiology* **27,** 561–575.

Dongmann G., Nurnberg H.W., Forstel H. & Wagener K. (1974) Enrichment of $H_2{}^{18}O$ in leaves of transpiring plants. *Radiation and Environmental Biophysics* **11,** 41–52.

Ehleringer J.R., Roden J. & Dawson T.E. (2000) Assessing ecosystem-level water relations through stable isotope ratio analysis. In *Methods in Ecosystem Science* (eds O. Sala, R. Jackson, H.A. Mooney & R. Howarth), pp. 181–198. Springer Verlag, New York, NY, USA.

Epstein S. & Yapp C. (1977) Isotope tree thermometers. *Nature* **266,** 477–478.

Farquhar G.D. & Cernusak L.A. (2005) On the isotopic composition of leaf water in the non-steady state. *Functional Plant Biology* **32,** 293–303.

Farquhar G.D. & Gan K.S. (2003) On the progressive enrichment of the oxygen isotopic composition of water along a leaf (Reprinted from *Plant, Cell & Environment* **26**, 801–819, 2003). *Plant, Cell & Environment* **26,** 1579–1597.

Farquhar G.D. & Lloyd J. (1993) Carbon and oxygen isotope effects in the exchange of carbon dioxide between terrestrial plants and the atmosphere. In *Stable Isotopes and Plant Carbon-Water Relations* (eds J.R. Ehleringer, A.E. Hall & G.D. Farquhar), pp. 47–70. Academic Press, San Diego, CA, USA.

Farquhar G.D., Ehleringer J.R. & Hubick K.T. (1989) Carbon isotope discrimination and photosynthesis. *Annual Review of Plant Physiology and Plant Molecular Biology* **40,** 503–537.

Farquhar G.D., Lloyd J., Taylor J.A., Flanagan L.B., Syvertsen J.P., Hubick K.T., Wong S.C. & Ehleringer J.R. (1993) Vegetation effects on the isotope composition of oxygen in atmospheric CO_2. *Nature* **363,** 439–443.

Farquhar G.D., Cernusak L.A. & Barnes B. (2007) Heavy water fractionation during transpiration. *Plant Physiology* **143,** 11–18.

Fisher J.B., Baldocchi D.D., Misson L., Dawson T.E. & Goldstein A.H. (2007) What the towers don't see at night: nocturnal sap flow in trees and shrubs at two AmeriFlux sites in California. *Tree Physiology* **27,** 597–610.

Flanagan L.B. & Ehleringer J.R. (1991) Effects of mild water-stress and diurnal changes in temperature and humidity on the stable oxygen and hydrogen isotopic composition of leaf water in *Cornus-Stolonifera* L. *Plant Physiology* **97,** 298–305.

Flanagan L.B., Comstock J.P. & Ehleringer J.R. (1991) Comparison of modeled and observed environmental-influences on the stable oxygen and hydrogen isotope composition of leaf water in *Phaseolus-Vulgaris* L. *Plant Physiology* **96,** 588–596.

Gat J.R. (1996) Oxygen and hydrogen isotopes in the hydrologic cycle. *Annual Review of Earth and Planetary Sciences* **24,** 225–262.

Gates D.M. (1980) *Biophysical Ecology*. Springer-Verlag, New York, NY, USA.

Griffis T.J., Baker J.M., Sargent S.D., Tanner B.D. & Zhang J. (2004) Measuring field-scale isotopic CO_2 fluxes with tunable diode laser absorption spectroscopy and micrometeorological techniques. *Agricultural and Forest Meteorology* **124,** 15–29.

Griffis T.J., Baker J.M. & Zhang J. (2005a) Seasonal dynamics and partitioning of isotopic CO_2 exchange in C-3/C-4 managed ecosystem. *Agricultural and Forest Meteorology* **132,** 1–19.

Griffis T.J., Lee X., Baker J.M., Sargent S.D. & King J.Y. (2005b) Feasibility of quantifying ecosystem-atmosphere (COO)-O-18-O-16 exchange using laser spectroscopy and the flux-gradient method. *Agricultural and Forest Meteorology* **135,** 44–60.

Griffis T.J., Zhang J., Baker J.M., Kljun N. & Billmark K. (2007) Determining carbon isotope signatures from micrometeorological measurements: implications for studying biosphere-atmosphere exchange processes. *Boundary-Layer Meteorology* **123,** 295–316.

Harwood K.G., Gillon J.S., Griffiths H. & Broadmeadow M.S.J. (1998) Diurnal variation of Delta(CO_2)-C-13, Delta(COO)-O-18-O-16 and evaporative site enrichment of delta(H_2O)-O-18 in Piper aduncum under field conditions in Trinidad. *Plant, Cell & Environment* **21,** 269–283.

Helliker B.R. & Griffiths H. (2007) Towards a plant-based proxy for the isotope ratio of atmospheric water vapor. *Global Change Biology* **13,** 723–733.

Helliker B.R., Roden J.S., Cook C. & Ehleringer J.R. (2002) A rapid and precise method for sampling and determining the oxygen isotope ratio of atmospheric water vapor. *Rapid Communications in Mass Spectrometry* **16,** 929–932.

Herbin H., Hurtmans D., Turquety S., Wespes C., Barret B., Hadji-Lazaro J., Clerbaux C. & Coheur P.F. (2007) Global distributions of water vapour isotopologues retrieved from IMG/ADEOS data. *Atmospheric Chemistry and Physics* **7,** 3957–3968.

Hoffmann G., Cuntz M., Weber C. *et al*. (2004) A model of the Earth's Dole effect. *Global Biogeochemical Cycles* **18,** GB1008, doi:1010.1029/2003GB002059.

IAEA/WMO (2004) *Stable Isotope Hydrology: Deuterium and Oxygen-18 in the Water Cycle*. (eds J.R. Gat & R. Gonfiantini), Technical Report Series No. 210, IAEA, Vienna 1981.

Lai C.T., Ehleringer J.R., Bond B.J. & U K.T.P (2006) Contributions of evaporation, isotopic non-steady state transpiration and atmospheric mixing on the delta O-18 of water vapour in Pacific

Northwest coniferous forests. *Plant, Cell & Environment* **29,** 77–94.

Lee X., Smith R. & Williams J. (2006) Water vapor $^{18}O/^{16}O$ isotope ratio in surface air in New England, USA. *Tellus* **58B,** 293–304.

Lee X., Kim K. & Smith R. (2007) Temporal variations of the $^{18}O/^{16}O$ signal of the whole-canopy transpiration in a temperate forest. *Global Biogeochemical Cycles* **21,** GB3013, doi:3010.1029/2006GB002871.

Lee X.H., Sargent S., Smith R. & Tanner B. (2005) In situ measurement of the water vapor O-18/O-16 isotope ratio for atmospheric and ecological applications. *Journal of Atmospheric and Oceanic Technology* **22,** 555–565.

Majoube M. (1971) Oxygen-18 and deuterium fractionation between water and steam. *Journal De Chimie Physique Et De Physico-Chimie Biologique* **68,** 1423–1436.

Monteith J.L. (1965) Evaporation and environment. In *The State and Movement of Water in Living Organisms* (ed. G.E. Fogg), pp. 1–47. Academic Press, New York, NY, USA.

Ogée J., Peylin P., Cuntz M., Bariac T., Brunet Y., Berbigier P., Richard P. & Ciais P. (2004) Partitioning net ecosystem carbon exchange into net assimilation and respiration with canopy-scale isotopic measurements: an error propagation analysis with (CO2)-C-13 and (COO)-O-18 data. *Global Biogeochemical Cycles* **18,** GB2019, doi:2010.1029/2003GB002166.

Ogée J., Cuntz M., Peylin P. & Bariac T. (2007) Non-steady-state, non-uniform transpiration rate and leaf anatomy effects on the progressive stable isotope enrichment of leaf water along monocot leaves. *Plant, Cell & Environment* **30,** 367–387.

Ometto J.P.H., Flanagan L.B., Martinelli L.A. & Ehleringer J.R. (2005) Oxygen isotope ratios of waters and respired CO_2 in Amazonian forest and pasture ecosystems. *Ecological Applications* **15,** 58–70.

Pendall E., Williams D.G. & Leavitt S.W. (2005) Comparison of measured and modeled variations in pinon pine leaf water isotopic enrichment across a summer moisture gradient. *Oecologia* **145,** 605–618.

Riley W.J., Still C.J., Helliker B.R., Ribas-Carbo M. & Berry J.A. (2003) O-18 composition of CO_2 and H_2O ecosystem pools and fluxes in a tallgrass prairie: simulations and comparisons to measurements. *Global Change Biology* **9,** 1567–1581.

Ripullone F., Matsuo N., Stuart-Williams H., Wong S.C., Borghetti M., Tani M. & Farquhar G. (2008) Environmental effects on oxygen isotope enrichment of leaf water in cotton leaves. *Plant Physiology* **146,** 729–736.

Roden J.S. & Ehleringer J.R. (1999) Observations of hydrogen and oxygen isotopes in leaf water confirm the Craig-Gordon model under wide-ranging environmental conditions. *Plant Physiology* **120,** 1165–1173.

Roden J.S., Lin G.G. & Ehleringer J.R. (2000) A mechanistic model for interpretation of hydrogen and oxygen isotope ratios in tree-ring cellulose. *Geochimica et Cosmochimica Acta* **64,** 21–35.

Saurer M., Siegwolf R. & Scheidegger Y. (2001) Canopy gradients in delta O-18 of organic matter as ecophysiological tool. *Isotopes in Environmental and Health Studies* **37,** 13–24.

Seibt U., Wingate L., Berry J.A. & Lloyd J. (2006) Non-steady state effects in diurnal O-18 discrimination by *Picea sitchensis* branches in the field. *Plant, Cell & Environment* **29,** 928–939.

Shuttleworth W.J. & Wallace J.S. (1985) Evaporation from sparse crops – an energy combination theory. *Quarterly Journal of the Royal Meteorological Society* **111,** 839–855.

Walker C.D., Leaney F.W., Dighton J.C. & Allison G.B. (1989) The influence of transpiration on the equilibration of leaf water with atmospheric water-vapor. *Plant, Cell & Environment* **12,** 221–234.

Wang X.F. & Yakir D. (1995) Temporal and spatial variations in the oxygen-18 content of leaf water in different plant species. *Plant, Cell & Environment* **18,** 1377–1385.

Wang X.F. & Yakir D. (2000) Using stable isotopes of water in evapotranspiration studies. *Hydrological Processes* **14,** 1407–1421.

Wen X.F., Sun X.M., Zhang S.C., Yu G.R., Sargent S.D. & Lee X. (2008) Continuous measurement of water vapor D/H and O-18/O-16 isotope ratios in the atmosphere. *Journal of Hydrology* **349,** 489–500.

White J.W.C., Lawrence J.R. & Broecker W.S. (1994) Modeling and interpreting D/H ratios in tree-rings – a test-case of White-Pine in the northeastern United-States. *Geochimica et Cosmochimica Acta* **58,** 851–862.

Worden J., Bowman K., Noone D., *et al*. (2006) Tropospheric emission spectrometer observations of the tropospheric HDO/H_2O ratio: estimation approach and characterization. *Journal of Geophysical Research-Atmospheres* **111,** D16309, doi:16310.11029/12005JD006606.

Yakir D. & Sternberg L.D.L. (2000) The use of stable isotopes to study ecosystem gas exchange. *Oecologia* **123,** 297–311.

Yakir D. & Wang X.F. (1996) Fluxes of CO_2 and water between terrestrial vegetation and the atmosphere estimated from isotope measurements. *Nature* **380,** 515–517.

Yakir D., Berry J.A., Giles L. & Osmond C.B. (1994) Isotopic heterogeneity of water in transpiring leaves – identification of the component that controls the delta-O-18 of atmospheric O-2 and CO_2. *Plant, Cell & Environment* **17,** 73–80.

Received 13 September 2007; received in revised form 8 February 2008; accepted for publication 28 April 2008

